A Knowledge Acquisition Method for Consumer Electronics Based on Triadic Hesitant Fuzzy Concept

Xianwei Xin, Ye Zhao, Chenyang Wang*, *Member, IEEE*,
Jiucheng Xu, Tarik Taleb, *Senior Member, IEEE*

***Abstract*—With the growing intelligence and personalization of consumer electronic products, extracting effective information has become a key challenge in Consumer Electronics (CE). Triadic Concept Analysis (TCA), an important extension of Formal Concept Analysis (FCA), is widely applied but often struggles to handle the hesitant fuzzy characteristics in real-world data. To address this gap, we propose a Triadic Hesitant Fuzzy Concept (THFC) model. First, we introduce the concept of a triadic hesitant fuzzy background, integrating the fuzzy and hesitant nature of data in the CE environment. We propose a knowledge acquisition method based on THFC, which constructs a multi-granularity knowledge space with a dynamic adjustment mechanism. This method captures subtle distinctions between different types of information and their hierarchical structures in the context of CE, offering significant support for knowledge discovery and decision-making in complex environments. Building on this, we design a variable-precision hybrid similarity measurement (VP-HSM) method to extract core, adjunct, and edge concepts, thus providing more precise and structured knowledge for data analysis and decision-making in CE. Experimental results on publicly available datasets show that the proposed method significantly improves classification accuracy and stability, effectively handling hesitant fuzzy data and improving the accuracy of concept extraction.**

***Index Terms*—Consumer electronics conceptual knowledge, similarity measurement, hesitation fuzzy set, triadic concept analysis, triadic hesitant fuzzy concept.**

I. Introduction

IN Consumer Electronics (CE), intelligent decision-making [1], [2], data analysis [3], intelligent computing [4], [5], and optimization programming [6], [7] have become central drivers of technological innovation and application progress. As device functions grow more complex, traditional methods struggle to effectively manage the increasing volume of data characterized by uncertainty, leading to the growing adoption of Fuzzy Logic Systems (FLS) [8]. However, when FLS is applied to address issues in CE, the results are often influenced by complex computations and variations in multiple rules, mainly due to compatibility and adaptability challenges across different devices. Therefore, integrating methods such as FLS to meet the complex demands of CE and achieve performance optimization remains a critical area of current research.

Triadic Concept Analysis (TCA) [9], as a significant extension of Formal Concept Analysis [10], enhances the ability to model complex data structures by introducing a third-dimensional conditional context. TCA constructs a hierarchical framework of concepts that includes objects, attributes, and conditions, systematically uncovering the intrinsic relationships between objects and attributes while enabling in-depth analysis of triadic associations. To date, TCA has been applied to various domains, including data mining [11], text analysis [12], decision support [13], and rule extraction [14].

As research on TCA advances, numerous scholars have actively explored and developed new paradigms. Regarding computational frameworks, Ignatov et al. [15] defined "optimal patterns" in triadic data, evaluating performance regarding resource efficiency, noise tolerance, and other criteria. Wan et al. [16] extended Multi-Granularity Formal Concept Analysis to three-dimensional data, optimizing multi-level data structures. Peng et al. [17] introduced the Z-TCA algorithm with Zero-Suppressed Decision Diagrams, achieving a threefold efficiency improvement over traditional algorithms. In theory, Bazin et al. [18] generalized Boolean concept lattices in the triadic context, addressing the lack of extremality properties. In applications, Ruas et al. [19] applied TCA to spatiotemporal variation analysis in the product lifecycle, while Kaytoue et al. [20] utilized TCA for biclustering in numerical data. Fei et al. [21] introduced a TCA-based dynamic k-clique detection method for analyzing evolving k-clique structures in dynamic social networks.

In practice, effective modeling and knowledge discovery for data with fuzziness and imprecision pose significant challenges in both theoretical research and real-world applications. To construct fuzzy granular concept clustering spaces and lower and upper approximation spaces, Deng et al. [22] introduced fuzzy attribute granular concepts, efficiently supporting label prediction in incremental learning. Elhady et al. [23] combined the fuzzy min-max algorithm with formal concept analysis to

This work is supported by the International Chinese Language Education Research Program (Grants No. 21YH18B, No. 23YH26C), the National Natural Science Foundation of China (Grant No. 62406104), the Key Research Project for Higher Education Institutions in Henan Province (Grants No. 24A520019 and No. 25A520029), the Henan Province Key Research and Development Project (Grant No. 251111210500), the Science and Technology Research Project of Henan Province (Grants No. 252102210056, No. 252102211013 and No. 242102210103), and in part by the National Social Science Foundation of Social Science Academic Associations Theme Academic Activities (Grant No. 23STA031).

X. Xin and Y. Zhao are with the school of Computer and Information Engineering, Henan Normal University, Xinxiang, 453007, China. X. Xin is also with the Key Laboratory of Computational Intelligence and Chinese Information Processing of Ministry of Education, 237016, Taiyuan, China (e-mail: xinxianwei@mail.bnu.edu.cn; zhaoye2023@stu.htu.edu.cn).

J. Xu is with the Key Laboratory of Artificial Intelligence and Personalized Learning in Education of Henan Province, Henan Province 453007, China (e-mail: xjc@htu.cn).

C. Wang is with the School of College of Shenzhen University, Computer and Software Engineering, Shenzhen, 518060, Guangdong, China (e-mail: chenyangwang@ieee.org).

T. Taleb is with the Faculty of Electrical Engineering and Information Technology, Ruhr University Bochum, 44801 Bochum, Germany (e-mail: tarik.taleb@rub.de).

*Chenyang Wang is the corresponding author (chenyangwang@ieee.org).

design a fuzzy iceberg lattice structure, significantly reducing computational costs in association rule mining. Belohlavek et al. [24] extended TCA's traditional framework by introducing fuzzy descriptions of relationships between objects, attributes, and conditions, further developing related theories and applications. This research has significantly expanded the boundaries of TCA theory and its practical applications.

However, data in CE exhibit considerable complexity and uncertainty, *e.g.,* interaction data from smart home devices can show instability or volatility due to environmental variations, while the behavioral responses of these devices, such as fluctuations in the activity patterns of smart light bulbs, often present uncertain, dynamically evolving, and non-deterministic characteristics. Consequently, addressing the challenges posed by fuzzy, dynamic variability and decision-making hesitancy in such data has become a critical issue in CE.

Redundancy often occurs in generating triadic concepts, making extracting core concepts crucial for triadic relationship analysis. Its effectiveness impacts concept quality. Existing studies address redundancy through concept reduction, minimizing unnecessary computations and information redundancy. However, this approach has limitations in core concept extraction, as it overlooks more profound semantic differences, leading to the extraction of core concepts based on superficial features with high computational costs. Analyzing intrinsic relationships through similarity measurement and optimizing concept selection can reduce complexity, improving efficiency and accuracy. This provides a more efficient solution for analyzing complex data in dynamic environments like smart homes and the Internet of Things in CE.

Based on these considerations, this paper combines Hesitant Fuzzy Sets (HFS) [25] with TCA to propose the Triadic Hesitant Fuzzy Concept (THFC) model. This model effectively captures the fuzziness and hesitation in object attribute values under different conditions, constructing a multi-granularity space based on the degree of affiliation and hesitancy. It mines the concepts of CE at varying granularities, thereby meeting the multi-scale knowledge acquisition needs in complex data environments. Moreover, traditional concept similarity measures often overlook the inherent hesitancy present in the data itself. In this paper, we propose a novel variable-precision hybrid similarity measurement (VP-HSM) method that integrates an improved Dice [26] coefficient with a Hausdorff [27] distance-based metric, grounded in Huffman's concept tree space. This approach combines the geometric distribution properties with conceptual intersections, offering a new methodology and tool for evaluating THFC similarity. The main contributions of this paper are as follows:

1) We introduce a triadic hesitant fuzzy context to address the fuzziness and hesitancy inherent in CE environments, along with the corresponding concept extraction method.
2) By constructing a multi-granularity knowledge space with a dynamic adjustment mechanism, we develop a hierarchical representation of conceptual knowledge tailored for CE.
3) We propose a VP-HSM for THFC and outline methods for extracting core, adjunct, and edge concepts within CE data environments.

The manuscript is structured as follows: Section II utilizes pertinent theoretical frameworks and conceptual underpinnings critical to the proposed methodology. Section III proposes the THFC construction and knowledge acquisition method. Section IV validates the proposed method through experimental results. Finally, Section V concludes the paper, discusses limitations, and outlines future research directions.

II. Basic Notions

A. Hesitant Fuzzy Sets

Definition 1. [28] Let U be a given non-empty finite set. $\forall X \subseteq U$, A fuzzy sets $\widetilde{G}$ is defined as a mapping from X to the interval $[0,1]$. Specifically, it can be expressed as:

$$\widetilde{G} = \{(x, \mu_{\widetilde{G}}(x)) \mid x \in X, \mu_{\widetilde{G}}(x) \in [0,1]\}, \tag{1}$$

where each element $x \in X$ is assigned a membership degree $\mu_{\widetilde{G}}(x) \in [0,1]$. The membership function represents the degree of membership of the element x in the fuzzy set $\widetilde{G}$.

Definition 2. [29] Let U be a given non-empty finite set. $\forall X \subseteq U$, an HFS on X is a subset mapping function from X to $[0,1]$, expressed as:

$$\widetilde{E} = \{(x, h_{\text{HFS}}(x)) \mid x \in X\}, \tag{2}$$

where $h_{\text{HFS}}(x)$ represents the set of possible degrees to which $x \in X$ belongs to $\widetilde{E}$. For convenience, we refer to $h = h_{\text{HFS}}(x)$ as a hesitant fuzzy element.

Given any two HFSs $\widetilde{A}$ and $\widetilde{B}$, their complement, union, and intersection operations are defined as follows:

1) $\{\widetilde{A}^c = \langle x, 1 - \mu_{\widetilde{A}}(x)\rangle \mid x \in X\}$.
2) $\{\widetilde{A} \cup \widetilde{B} = \langle x, \max(\mu_{\widetilde{A}}(x), \mu_{\widetilde{B}}(x))\rangle \mid x \in X\}$.
3) $\{\widetilde{A} \cap \widetilde{B} = \langle x, \min(\mu_{\widetilde{A}}(x), \mu_{\widetilde{B}}(x))\rangle \mid x \in X\}$.

B. Triadic Fuzzy Concept

Definition 3. [9] Let the quadruple (U, A, C, I) be a triadic formal context, where U, A, and C are non-empty finite sets, and $I \subseteq U \times A \times C$ represents the triadic relationship between the sets U, A, and C. We define U, A, and C as the set of objects, the set of attributes, and the set of conditions, respectively, with the elements of these sets referred to as objects, attributes, and conditions. For every $\forall x \in U, \forall a \in A$ and $\forall c \in C$, if there exists a triadic relationship I between object x, attribute a, and condition c, we write $(x, a, c) \in I$, meaning that object x has attribute a under condition c.

Definition 4. [9] Let (U, A, C, I) be a triadic formal context, and let $X \subseteq U$, $B \subseteq A$, and $D \subseteq C$. The following rules apply:

Case 1: In the projection formal context (A, C, I_X), the operators $B^{(X,\cdot,\cdot)}$ and $D^{(X,\cdot,\cdot)}$ are defined as:

$$\begin{aligned} B^{(X,\cdot,\cdot)} &= \{c \in C \mid \forall a \in B, (a,c) \in I_X\}, \\ D^{(X,\cdot,\cdot)} &= \{a \in A \mid \forall c \in D, (a,c) \in I_X\}. \end{aligned} \tag{3}$$

Case 2: In the projection formal context (U, C, I_B), the operators $X^{(\cdot,B,\cdot)}$ and $D^{(\cdot,B,\cdot)}$ are defined as:

$$\begin{aligned} X^{(\cdot,B,\cdot)} &= \{c \in C \mid \forall x \in X, (x,c) \in I_B\}, \\ D^{(\cdot,B,\cdot)} &= \{x \in U \mid \forall c \in D, (x,c) \in I_B\}. \end{aligned} \tag{4}$$

Case 3: In the projection formal context (U, A, I_D), the operators $X^{(\cdot,\cdot,D)}$ and $B^{(\cdot,\cdot,D)}$ are defined as:

$$\begin{aligned} X^{(\cdot,\cdot,D)} &= \{a \in A \mid \forall x \in X, (x,a) \in I_D\}, \\ B^{(\cdot,\cdot,D)} &= \{x \in U \mid \forall a \in B, (x,a) \in I_D\}. \end{aligned} \tag{5}$$

Definition 5. [9] Let (U, A, C, I) be a triadic formal context. For any $X \subseteq U$, $B \subseteq A$, and $D \subseteq C$, if the following conditions are satisfied: $B = D^{(X,\cdot,\cdot)}$, $D = B^{(X,\cdot,\cdot)}$, $X = D^{(\cdot,B,\cdot)}, D = X^{(\cdot,B,\cdot)}$, $X = B^{(\cdot,\cdot,D)}$, $B = X^{(\cdot,\cdot,D)}$, then the triple (X, B, D) is called a *triadic concept* of the triadic formal context (U, A, C, I). In this case, X, B, and D are the extents, intents and moduses of the triadic concept (X, B, D), respectively. To better address the uncertainty in real-world data, Belohlávek [24] extended the concept of triadic fuzzy formal contexts by introducing fuzzy set theory.

Definition 6. [24] Let $(U, A, C, \widetilde{I} = \phi(U \times A \times C))$ be a triadic fuzzy formal context, where $\widetilde{I}$ represents the triadic fuzzy relation between the object set U, the attribute set A, and the condition set C. In this relation, each element has a membership degree $\mu \in [0, 1]$, which indicates the degree of membership of an object x to an attribute a under a given condition c. Moreover, a threshold ∂ is considered. In the projection formal contexts $(A, C, \widetilde{I}_X), (U, C, \widetilde{I}_B)$ and $(U, A, \widetilde{I}_D)$, for any $X \subseteq U, B \subseteq A, D \subseteq C$, we have the following:

$$\begin{aligned} \widetilde{B}^{(X,\cdot,\cdot)} &= \{c \in C \mid \forall a \in B, \mu(a,c) \geq \partial\}, \\ \widetilde{D}^{(X,\cdot,\cdot)} &= \{a \in A \mid \forall c \in D, \mu(a,c) \geq \partial\}, \\ \widetilde{X}^{(\cdot,B,\cdot)} &= \{c \in C \mid \forall x \in X, \mu(x,c) \geq \partial\}, \\ \widetilde{D}^{(\cdot,B,\cdot)} &= \{x \in U \mid \forall c \in D, \mu(x,c) \geq \partial\}, \\ \widetilde{X}^{(\cdot,\cdot,D)} &= \{a \in A \mid \forall x \in X, \mu(x,a) \geq \partial\}, \\ \widetilde{B}^{(\cdot,\cdot,D)} &= \{x \in U \mid \forall a \in B, \mu(x,a) \geq \partial\}. \end{aligned} \tag{6}$$

Definition 7. [24] Let $(U, A, C, \widetilde{I} = \phi(U \times A \times C))$ be a triadic fuzzy formal context. If the following conditions hold: $B = \widetilde{D}^{(X,\cdot,\cdot)}$, $D = \widetilde{B}^{(X,\cdot,\cdot)}$, $X = \widetilde{D}^{(\cdot,B,\cdot)}, D = \widetilde{X}^{(\cdot,B,\cdot)}$, $X = \widetilde{B}^{(\cdot,\cdot,D)}$, $B = \widetilde{X}^{(\cdot,\cdot,D)}$, then the triple $(\phi(X), B, D)$ is called a *triadic fuzzy concept* in the triadic fuzzy formal context $(U, A, C, \widetilde{I})$. Where, $\phi(X)$ is a fuzzy set defined on X, where each object $x \in X$ has a membership degree:$\mu(x) = \min_{a \in A} \mu(x, a, c)$.

III. Triadic Hesitant Fuzzy Concept and Knowledge Acquisition

The trading environment of CE is inherently complex. To effectively extract conceptual knowledge in this context, this section integrates the concepts of the Triangular Fuzzy Number (TFN) [30] and Hesitant Entropy (HE) [31], introducing the notion of the Triadic Hesitant Fuzzy Context (THFC). Furthermore, by leveraging multi-granularity theory, we propose a novel THFC-based multi-granularity knowledge acquisition method. This method utilizes a VP-HSM to extract core, adjunct, and edge THFCs. The overall framework is illustrated in Fig. 1.

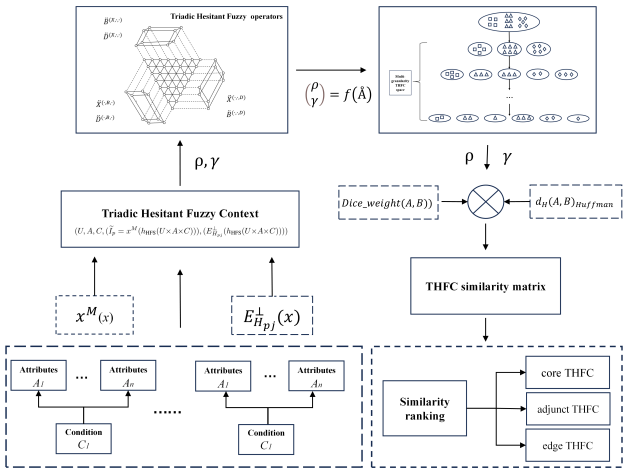

Fig. 1. THFC-based methodological framework for knowledge acquisition

A. Construction of Triadic Hesitant Fuzzy Concept

Definition 8. Let the quadruple $(U, A, C, \ddot{I})$ represent a Triadic Hesitant Fuzzy Context, where $\ddot{I}$ denotes the triadic hesitant fuzzy relations between the object set U and the attribute set A under the condition set C, $\ddot{I} = (x^M(h_{\text{HFS}}(U \times A \times C))), (E^{\perp}_{H_{pj}}(h_{\text{HFS}}(U \times A \times C)))$. Each element within these relations is associated with a membership degree x^M and HE $E^{\perp}_{H_{pj}}$, subject to thresholds ρ and γ. Under the projected Hesitant Fuzzy Contexts: $(A, C, \ddot{I}_X), (U, C, \ddot{I}_B)$ and $(U, A, \ddot{I}_D)$ for any subsets $X \subseteq U$, $B \subseteq A$, and $D \subseteq C$, we have:

$$\begin{aligned} \ddot{B}^{(X,\cdot,\cdot)} =& \{c \in C \mid \forall a \in B, x^M(h_{\text{HFS}}(a \times c)) \geq \rho \wedge \\ & E^{\perp}_{H_{pj}}(h_{\text{HFS}}(a \times c)) \leq \gamma\}, \\ \ddot{D}^{(X,\cdot,\cdot)} =& \{a \in A \mid \forall c \in D, x^M(h_{\text{HFS}}(a \times c)) \geq \rho \wedge \\ & E^{\perp}_{H_{pj}}(h_{\text{HFS}}(a \times c)) \leq \gamma\}, \\ \ddot{X}^{(\cdot,B,\cdot)} =& \{c \in C \mid \forall x \in X, x^M(h_{\text{HFS}}(x \times c)) \geq \rho \wedge \\ & E^{\perp}_{H_{pj}}(h_{\text{HFS}}(x \times c)) \leq \gamma\}, \\ \ddot{D}^{(\cdot,B,\cdot)} =& \{x \in U \mid \forall c \in D, x^M(h_{\text{HFS}}(x \times c)) \geq \rho \wedge \\ & E^{\perp}_{H_{pj}}(h_{\text{HFS}}(x \times c)) \leq \gamma\}, \\ \ddot{X}^{(\cdot,\cdot,D)} =& \{a \in A \mid \forall x \in X, x^M(h_{\text{HFS}}(x \times a)) \geq \rho \wedge \\ & E^{\perp}_{H_{pj}} \leq \gamma\}, \\ \ddot{B}^{(\cdot,\cdot,D)} =& \{x \in U \mid \forall a \in B, x^M(h_{\text{HFS}}(x \times a)) \geq \rho \wedge \\ & E^{\perp}_{H_{pj}}(h_{\text{HFS}}(x \times a)) \leq \gamma\}, \end{aligned} \tag{7}$$

where $0 \leq x^M \leq 1$ and $0 \leq E^{\perp}_{H_{pj}} \leq 1$.

Definition 9. Let the quadruple $(U, A, C, \ddot{I})$ represent a Triadic Hesitant Fuzzy Context. If the following equalities hold: $B = \ddot{D}^{(X,\cdot,\cdot)}, D = \ddot{B}^{(X,\cdot,\cdot)}, X = \ddot{D}^{(\cdot,B,\cdot)}, D = \ddot{X}^{(\cdot,B,\cdot)}, X = \ddot{B}^{(\cdot,\cdot,D)}, B = \ddot{X}^{(\cdot,\cdot,D)}$, then the triple $(\psi(X), B, D)$ is called a THFC over the Triadic Hesitant Fuzzy Context $(U, A, C, \ddot{I})$. For simplicity, all triadic hesitant fuzzy concepts over U are denoted as $\mathcal{T}$.

If $\psi(X)$ is a hesitant fuzzy relational set on X, then: $\psi(X) = \{(x_1, \mathcal{H}(x_1), E(x_1))), \ldots, (x_n, \mathcal{H}(x_n), E(x_n))) \mid x_i \in X\}$, where $\mathcal{H} = \min_{a \in A, c \in D} x^M(h_{\text{HFS}}(x \times a \times c)), E = \max_{a \in A, c \in D} E^{\perp}_{H_{pj}}(h_{\text{HFS}}(x \times a \times c))$.

In practical applications, the parameters ρ and γ in Equation (7) can be viewed as granular judgment conditions. The pseudocode for generating Triadic THFCs is presented in Algorithm 1.

Algorithm 1 THFC Extraction Algorithm

Input: Hesitation entropy matrix HFE, Membership degree matrix MOD, threshold value γ, ρ
Output: THFCs $\mathcal{C}$
Initialize: $\mathcal{C} \leftarrow \emptyset$
for each cell $[i, j]$ in MOD **do**
  Replace $MOD[i, j]$ with x_m.
end for
for each cell $[i, j]$ in HFE **do**
  Parse $p = [p_1, p_2, p_3]$ and compute $E^{\perp}_{H_{pj}}$
  Replace $HFE[i, j]$ with $E^{\perp}_{H_{pj}}$.
end for
for $D \subseteq C$, $B \subseteq A$, $X \subseteq U$ **do**
  Compute:
  $\ddot{B}^{(X,\cdot,\cdot)}, \ddot{D}^{(X,\cdot,\cdot)}, \ddot{X}^{(\cdot,B,\cdot)}, \ddot{D}^{(\cdot,B,\cdot)}, \ddot{X}^{(\cdot,\cdot,D)}, \ddot{B}^{(\cdot,\cdot,D)}$.
  if $X = \ddot{D}^{(\cdot,B,\cdot)}, D = \ddot{X}^{(\cdot,B,\cdot)}, X = \ddot{B}^{(\cdot,\cdot,D)}, B = \ddot{X}^{(\cdot,\cdot,D)}$ **then**
    Add (X, B, D) to $\mathcal{C}$
  end if
end for
Return: $\mathcal{C}$

These parameters can be adjusted to suit specific downstream tasks, allowing for the selection of an appropriate level of granularity.

- **Coarse Granularity:** Suitable for early-stage exploration and global trend analysis, this level extracts a larger number of weakly associated THFCs.
- **Fine Granularity:** Ideal for precise decision-making and knowledge validation, it identifies key THFCs with higher semantic accuracy.
- **Medium Granularity:** Useful for comprehensive global analysis, this level strikes a balance between the quantity and quality of THFCs.

In the evaluation of CE, particularly for complex products such as mobile phones, the criteria and attributes involved often exhibit significant uncertainty. To address this, the following example demonstrates the process of extracting THFCs from a Triadic Hesitant Fuzzy Context. Table I presents a Triadic Hesitant Fuzzy Context, where x_1, x_2, and x_3 represent three types of consumer electronic products: high-end, mid-range, and entry-level, respectively. S_1, S_2, and S_3 denote the performance attributes of mobile phones, while C_1 and C_2 represent two evaluation criteria. With the thresholds set to $\rho = 0.6$, $\gamma = 0.35$. Algorithm 1 generates 8 THFCs, as presented in Table II.

B. Variable-Precision Hybrid Similarity Measurement

To improve the accuracy and comprehensiveness of THFC similarity evaluation, this section introduces a Huffman Concept Tree to represent the hierarchical relationships among THFCs and incorporates a Hesitant Fuzzy Weighted Dice Coefficient to measure the hesitant fuzzy information within them.

Definition 10. For $\forall L$ and $l \in \mathcal{T}$, the Hausdorff distance in the metric space of the Huffman Concept Tree is expressed as:

$$d_H(L,l)_{\text{Huffman}} = \max\left\{ \sup_{\dot{a}\in L}\inf_{\dot{b}\in l} d_{\text{Huffman}}(\dot{a},\dot{b}), \sup_{\dot{b}\in l}\inf_{\dot{a}\in L} d_{\text{Huffman}}(\dot{a},\dot{b}) \right\}. \tag{8}$$

By encoding the concept granule frequencies in L and l as Huffman codes, a Huffman Concept Tree is constructed. The path lengths within the tree are then used to measure the semantic distance between concepts, replacing the traditional Euclidean distance in similarity measures. This approach prioritizes high-frequency concept granules for encoding, enhancing the semantic differentiation between critical concepts and improving the efficiency of the measurement process.

Definition 11. For $\forall L$ and $l \in \mathcal{T}$, the Hesitant Fuzzy Weighted Dice Coefficient is defined as:

$$\begin{aligned}\text{Dice}_{\text{weight}}(L,l) = \omega\frac{\sum_{\dot{x}\in L\cap l}\left(x_L^M(\dot{x}) + x_l^M(\dot{x})\right)}{\sum_{\dot{a}\in L} x_L^M(\dot{a}) + \sum_{\dot{b}\in l} x_l^M(\dot{b})} + \\ (1-\omega)\frac{\sum_{\dot{x}\in L\cap l}\left(E_L(\dot{x}) + E_l(\dot{x})\right)}{\sum_{\dot{a}\in L} E_L(\dot{a}) + \sum_{\dot{b}\in l} E_l(\dot{b})},\end{aligned} \tag{9}$$

where $\omega \in [0,1]$ is the hesitant fuzzy weighting coefficient, $x_L^M(\dot{a})$ and $x_l^M(\dot{b})$ represent the membership degrees of concept granules $\dot{a} \in L$ and $\dot{b} \in l$, respectively. Similarly, $E_L(\dot{a})$ and $E_l(\dot{b})$ denote the hesitation entropy of concept granules $\dot{a} \in L$ and $\dot{b} \in l$, respectively. $x_L^M(\dot{x})$, $x_l^M(\dot{x})$, $E_L(\dot{x})$, and $E_l(\dot{x})$ correspond to the minimum membership degrees and maximum hesitation entropy for the intersecting concept granules between the two THFCs.

Equation (9) comprehensively captures the importance differences and uncertainties among concept granules within the concept sets, offering a more accurate representation and handling of fuzzy and hesitant information in the data. Accordingly, the VP-HSM for THFCs is expressed as:

$$D_{\text{HTDH}}(L,l) = \frac{e^{-d_H(L,l)_{\text{Huffman}}/100}\cdot \text{Dice}_{\text{weight}}(L,l)}{1+\theta\left(d_H(L,l)_{\text{Huffman}}\right)^2}, \tag{10}$$

where $\theta \in [0,1]$ is the weighting parameter for difference. The results of Equation (10) are influenced by the hesitant fuzzy weighting coefficient ω and the weighting parameter θ. As shown in Fig. 2, adjusting these parameters reveals significant nonlinear characteristics.

Theorem 1. For $\forall L, l$ and $\xi \in \mathcal{T}$, their D_{HTDH} satisfies the following properties:

1) $0 \le D_{\text{HTDH}}(L,l) \le 1$,
2) $D_{\text{HTDH}}(L,l) = 1$ if $L = l$,
3) $D_{\text{HTDH}}(L,l) = D_{\text{HTDH}}(l,L)$,
4) $D_{\text{HTDH}}(L,\xi) \le D_{\text{HTDH}}(L,l)$ and $D_{\text{HTDH}}(L,\xi) \le D_{\text{HTDH}}(l,\xi)$ if $L \subseteq l \subseteq \xi$.

Proof: According to its nature, it is easily provable.

TABLE I
TRIADIC HESITANT FUZZY CONTEXT

	C_1			C_2		
	S_1	S_2	S_3	S_1	S_2	S_3
x_1	(0.3, 0.6, 0.8)	(0.4, 0.5, 0.8)	(0.1, 0.6, 0.9)	(0.4, 0.6, 0.6)	(0.2, 0.8, 0.9)	(0.4, 0.6, 0.8)
x_2	(0.7, 0.8, 0.9)	(0.2, 0.5, 0.9)	(0.1, 0.6, 0.8)	(0.1, 0.4, 0.6)	(0.1, 0.1, 0.2)	(0.8, 0.9, 0.9)
x_3	(0.5, 0.6, 0.6)	(0.1, 0.7, 1.0)	(0.4, 0.6, 0.7)	(0.6, 0.6, 0.7)	(0.1, 0.4, 0.8)	(0.1, 0.3, 0.3)

TABLE II
THFCS FROM THE ABOVE TABLE

THFCs	**Extents**	**Intents**	**Moduses**	**Triadic Diagram**
T_1	$\{(x_2, 0.8, 0.25), (x_3, 0.6, 0.11)\}$	S_1	c_1	
T_2	$\{(x_1, 0.6, 0.22), (x_3, 0.6, 0.14)\}$	S_1	c_2	
T_3	U	$\emptyset$	C	
T_4	$\{(x_3, 0.6, 0.14)\}$	S_1	c_1, c_2	
T_5	$\{(x_2, 0.9, 0.11)\}$	S_3	c_2	
T_6	U	A	$\emptyset$	
T_7	$\{(x_3, 0.6, 0.35)\}$	$\{S_1, S_3\}$	c_1	
T_8	$\emptyset$	A	C	

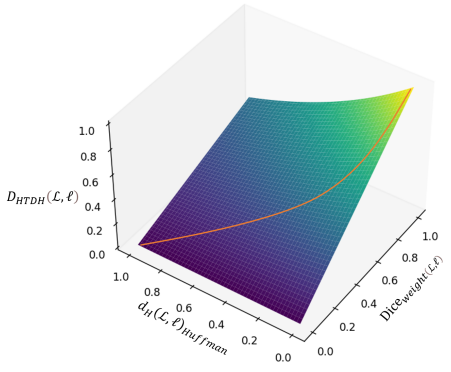

Fig. 2. VP-HSM trend analysis

Definition 12. Let $L = \{L_1, L_2, \ldots, L_{|L|}\}$ represent a set of THFCs, and let $l \in \mathcal{T}$ be a specific THFC. The mean value of the VP-HSM between L and l is defined as:

$$D_{\text{mean}}(L, l) = \frac{1}{|L|} \sum_{i=1}^{|L|} D_{\text{HTDH}}(L_i, l), \tag{11}$$

where $D_{\text{HTDH}}(L_i, l)$ denotes the VP-HSM between the i-th THFC L_i and l. This mean value provides an aggregate similarity score, capturing the overall relationship between the set L and the element l.

Based on the mean similarity scores D_{mean}, the THFCs in L can be categorized into three distinct groups: core, adjunct, and edge THFCs, defined as follows:

$$\text{Core}(L) = \left\{L_i \mid L_i \in L,\ i \leq \lceil \alpha |L| \rceil \right\}, \tag{12}$$

$$\text{Edge}(L) = \left\{L_i \mid L_i \in L,\ i > \lceil \beta |L| \rceil \right\}, \tag{13}$$

$$\text{Adjunct}(L) = \left\{L_i \mid L_i \in L,\ \lceil \alpha |L| \rceil < i \leq \lceil \beta |L| \rceil \right\}, \tag{14}$$

where, L_i denotes the i-th THFC in L, sorted in descending order of their D_{HTDH} scores. α is the proportion threshold for identifying core THFCs, and β is the proportion threshold for defining marginal THFCs. Furthermore, core THFCs represent the most relevant concepts, adjunct THFCs are moderately relevant, and edge THFCs have the least relevance, based on their D_{HTDH} scores.

The calculation process for the VP-HSM is outlined in Algorithm 2, which is summarized as follows:

Algorithm 2 THFC Similarity Calculation

Input: THFCs C, Parameters θ, ω
Output: Similarity Matrix M, core, edge, adjunct THFC K,N, p
Initialize: $M \leftarrow \emptyset$
for each pair of THFCs **do**
  $Compute: D_1 = \text{Dice}_{\text{weight}} = \omega \cdot \text{Dice}_1 + (1-\omega) \cdot \text{Dice}_2$
  $Compute: D_2 = \text{Hausdorff}_{\text{distance}}$
  if $D_2 = 0$ or $D_1 = 1$ **then**
    $M[i, j] \leftarrow 1$
  else
    $M[i, j] \leftarrow D_1 \cdot \exp(-D_2/100)/(1 + \theta \cdot D_2^2)$
  end if
end for
Similarity ordering then select
Return: M, K, N, p

IV. EXPERIMENTAL ANALYSIS

A. Experimental Setup

To evaluate the efficacy and robustness of the proposed approach, we conducted THFC extraction across seven publicly available datasets, identifying core, adjunct, and edge THFCs. Descriptions of the datasets used in this study are summarized in Table III. Except for the Diabetes dataset, which was obtained from Kaggle, all other datasets were sourced from the UCI Machine Learning Repository. The experimental environment is as follows: hardware configuration—Intel i7-9700 processor with 8.00 GB of RAM; software environment—64-bit Windows 10 operating system and PyCharm 5.0.3 IDE.

TABLE III
DESCRIPTION OF DATASETS

No.	Data	Attributes	Samples	Classes
1	Breast Cancer	9	699	2
2	Diabetes	8	768	2
3	Wine	13	178	3
4	Segmentation	19	2100	7
5	WPBC	33	198	2
6	Ionosphere	34	351	2
7	WDBC	30	569	2

B. Preprocessing and THFC Extraction

To improve the efficiency of THFC extraction, several data preprocessing steps were implemented. First, MinMaxScaler was applied to normalize the data, removing discrepancies in feature scales and ensuring consistency across all dimensions. Next, the K-means [32] was used to cluster the samples, with the silhouette coefficient [33] helping to determine the optimal K value for the best clustering performance. Additionally, the Monte Carlo simulation method [34] was employed to expand the dataset by simulating hesitant scenarios. Finally, each data element was represented as a TFN, offering a more flexible and comprehensive depiction of both fuzziness and hesitation. The THFC extraction was then carried out using Algorithm 1, and the detailed process is illustrated in Fig. 3.

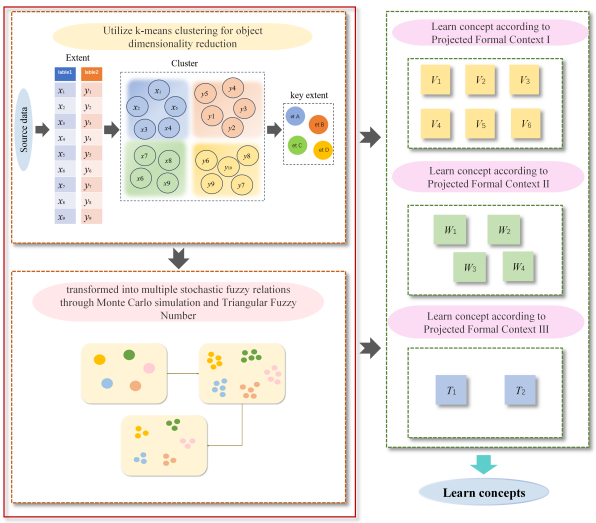

Fig. 3. Process diagram for extracting THFCs

Fig. 4 illustrates the number of THFCs across different granularity spaces. According to the figure, as ρ increases, the interaction criteria among target objects, attributes, and conditions become more stringent, reducing the number of extracted THFCs. Correspondingly, under these stricter conditions, the extracted THFCs exhibit higher semantic precision and representativeness. Similarly, increasing γ allows for greater hesitation, thereby expanding the number of extractable THFCs. However, due to the elevated entropy, the semantic clarity of these THFCs decreases. Conversely, reducing γ diminishes the number of THFCs while enhancing their semantic consistency and stability. According to Definition 9, Table IV validates the impact of different granularity spaces on the extraction of core and edge THFCs within the Diabetes dataset. Overall, the adjustment of granularity effectively balances the number and semantic accuracy of core and edge THFCs, offering a more refined optimization direction.

TABLE IV
DIFFERENT GRANULARITY SPACES ON THE EXTRACTION OF CORE AND EDGE THFCS WITHIN THE DIABETES DATASET.

ρ	γ	Core THFC	Edge THFC
0.5	0.45	$\{(x_1,x_2),(s_4),(c_1,c_2)\}$, $\{(x_1),(s_1,s_4),(c_1,c_2)\}$, $\{(x_1,x_2),(s_1,s_3,s_4),(c_1)\}$, $\{(x_1,x_2,x_7),(s_3,s_4),(c_1)\}$, $\{(x_1),(s_1,s_2,s_3),(c_1)\}$	$\{(x_4),(s_2,s_4),(c_1)\}$, $\{(x_3,x_4,x_5,x_6),(s_2),(c_1)\}$, $\{(x_5),(s_1,s_3),(c_2)\}$, $\{(x_1,x_4,x_5),(s_1),(c_2)\}$, $\{(x_1),(s_1,s_2,s_3),(c_1)\}$
0.55	0.40	$\{(x_1,x_2),(s_1,s_4),(c_1)\}$, $\{(x_2),(s_4),(c_1,c_2)\}$, $\{(x_3,x_4,x_6),(s_2),(c_1,c_2)\}$, $\{(x_3),(s_2),(c_1,c_2)\}$	$\{(x_5),(s_1,s_3),(c_2)\}$, $\{(x_1,x_4,x_5),(s_2),(c_1)\}$, $\{(x_6,x_7),(s_3),(c_1)\}$, $\{(x_4,x_6,x_7),(s_2),(c_2)\}$
0.60	0.35	$\{(x_1,x_5),(s_3),(c_1)\}$, $\{(x_1),(s_1,s_3),(c_1)\}$, $\{(x_5),(s_3,s_4),(c_1)\}$	$\{(x_6,x_7),(s_2),(c_2)\}$, $\{(x_7),(s_2),(c_1)\}$, $\{(x_5),(s_3,s_4),(c_1)\}$
0.65	0.30	$\{(x_4,x_7),(s_2),(c_2)\}$, $\{(x_4),(s_2),(c_1,c_2)\}$	$\{(x_7),(s_3),(c_1)\}$, $\{(x_5),(s_1),(c_2)\}$
0.70	0.25	$\{(x_5),(s_3),(c_1,c_2)\}$	$\emptyset$
0.75	0.20	$\{(x_6),(s_3),(c_2)\}$	$\emptyset$

TABLE V
COMPARISON OF AVERAGE PERFORMANCE WITH STATE-OF-THE-ART METHODS ON WINE DATASETS

Method	Classifier	Accuracy (%)	Number of Features
Hu et al. [37]	SVM	95.33	9
Hu et al. [41]	KNN	97.22	**5**
Sang et al. [42]	Random Tree	93.26	9
Wang et al. [43]	KNN	97.22	9
Huang et al. [44]	KNN	97.08	8
Zhan et al. [45]	CART	92.09	7
Wei et al. [46]	KNN	97.78	6
Zhao et al. [47]	KNN	96.05	9
Du et al. [48]	Bayes Net	94.4	11
Huang et al. [49]	KNN	97.14	9
Huang et al. [50]	KNN	97.06	8
Ours	KNN	**98.32**	6

C. Feature Selection and Performance Evaluation

The VP-HSM method proposed in this study aims to precisely evaluate the degree of similarity among THFCs, thereby facilitating the identification of core, adjunct, and edge THFCs within the THFC space. These identified concepts are then used as structured knowledge for feature selection. Specifically, attributes within core THFCs and adjunct THFCs are categorized as core and adjunct attributes, respectively, while attributes within edge THFCs, as well as those not belonging to any THFC, are considered edge attributes. To assess the adjunct attributes, we employ the XGBClassifier [35], treating them as supplementary information. The results of feature selection across seven datasets, based on Algorithm 2, along with the overall importance ranking of attributes, are presented in Table VI. Based on the ranking results in Table VI, attributes are sequentially added to the base classifiers KNN and SVM, and the corresponding evaluation metrics

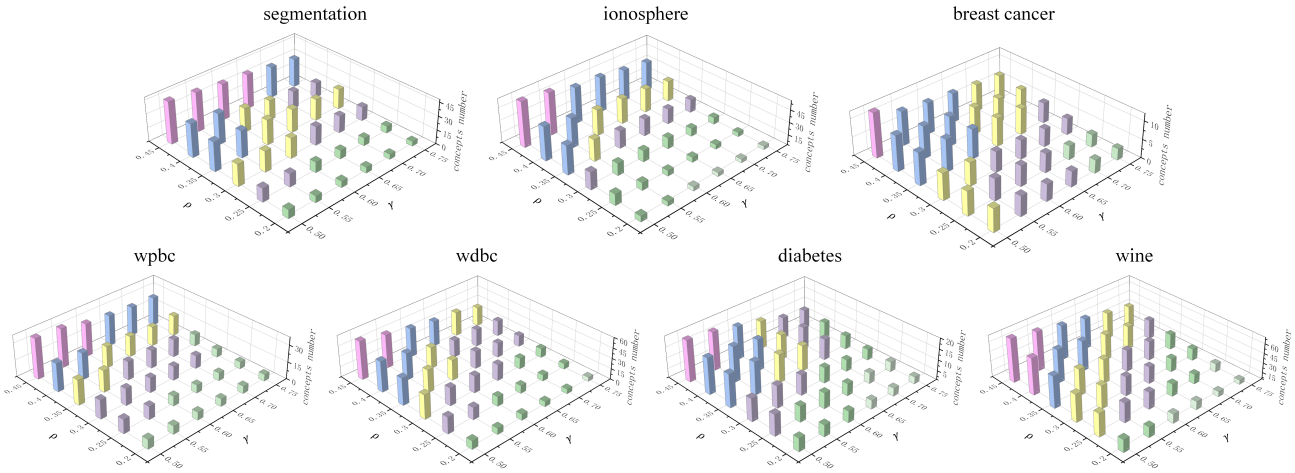

Fig. 4. The number of THFCs across different granularity spaces

TABLE VI
SORTING ATTRIBUTES BASED ON THE PROPOSED METHOD.

No.	Core Attributes	Edge Attributes	Overall Order of Attributes
1	3, 6, 4	8 ,5, 9	3, 6, 4, 2, 7, 1, 8, 5, 9
2	2, 6, 8	5, 1, 4	2, 6, 8, 7, 3, 4, 5, 1
3	1, 7, 10	9, 11, 12	1, 10, 7, 13, 4, 5, 6, 2, 3, 8, 9, 11, 12
4	10, 15, 11, 19	3, 4, 5, 9	10, 15, 19, 11, 14, 18, 12, 2, 16, 13, 17, 1, 8, 7, 6, 9, 4, 5, 3
5	1, 3, 22, 31	4, 17, 5, 24	3, 22, 1, 31, 33, 19, 2, 13, 29, 32, 28, 7, 12, 26, 18, 8, 23, 6, 11, 27, 20, 15, 10, 30, 14, 9, 25, 21, 16, 24, 4, 17, 5
6	5, 27, 7, 3, 1	10, 11, 12, 13, 14	5, 27, 7, 3, 1, 32, 9, 16, 8, 17, 6, 29, 4, 24, 20, 34, 22, 21, 28, 18, 30, 31, 26, 33, 25, 23, 19, 15, 2, 10, 11, 12, 13, 14
7	23, 21, 2, 7	20, 19, 18, 16, 15, 12, 10, 9	21, 23, 2, 7, 8, 28, 24, 4, 22, 27, 11, 17, 13, 25, 14, 26, 6, 30, 1, 5, 29, 3, 20, 19, 18, 16, 15, 12, 10, 9

are calculated: Accuracy $= \frac{\text{TP+TN}}{\text{TP+TN+FP+FN}}$, Precision $= \frac{\text{TP}}{\text{TP+FP}}$, Recall $= \frac{\text{TP}}{\text{TP+FN}}$, as illustrated in Fig. 5. With the sequential addition of attributes, the overall classification performance improves progressively and tends to converge. This demonstrates that the proposed method effectively mitigates the adverse effects of redundant and noisy attributes, thereby enhancing classification performance.

To validate the effectiveness of the proposed method, comparative experiments were conducted against several state-of-the-art approaches, as summarized in Table VII. The base classifier KNN(with K=3) was employed under a 10-fold cross-validation framework, The comparative results are presented in Table VIII, where the proposed method achieved average accuracies of 98.09%, 79.22%, 86.67%, 98.11%, 98.32%, 97.07%, and 98.26% across the Breast Cancer, Diabetes, WPBC, Ionosphere, Wine, WDBC, and Segmentation datasets, respectively. These results consistently outperformed the competing methods and demonstrated lower standard deviations, indicating the stability of the proposed method across various datasets. Overall, the proposed method achieved an average accuracy of 93.68% across all datasets, showcasing its strong classification capability.

Given the varying objectives of different research methodologies, the datasets selected are often closely related to their specific research content and characteristics, leading to certain differences. Among the diverse datasets, the Wine dataset is particularly notable for its clear structure, moderate number of features, and strong representativeness. Therefore, we conducted a comparative analysis of the classification performance on the Wine dataset, focusing on metrics such as classification accuracy and the number of selected features. The experimental results are presented in Table V.

D. Parameter Sensitivity Analysis

The parameters ω and θ respectively influence the calculation of $\text{Dice}_{\text{weight}}(A, B)$ and $d_H(A, B)_{\text{Huffman}}$. Specifically, $\omega \in [0, 1]$ serves as a weighting coefficient to balance the contributions of membership degree and hesitation entropy in $\text{Dice}_{\text{weight}}(A, B)$. By adjusting ω, the relative influence of these two factors can be dynamically fine-tuned to meet different similarity assessment requirements. Similarly, θ modulates the nonlinear scaling effect of $d_H(A, B)_{\text{Huffman}}$, where higher values of θ gradually reduce the impact of $d_H(A, B)_{\text{Huffman}}$ on the similarity measurement. To analyze the role and effects of these parameters under various configurations, experiments were conducted with different ranges of ω and θ. The results are illustrated in Fig. 6.

Fig. 6 shows 25 variation trends under different parameters for each dataset, and the variation is gradually obvious as the parameter difference becomes larger. Concretely, as the value of θ gradually increases, D_{HTDH} exhibits a slow downward trend overall. In contrast, parameter ω plays a more significant

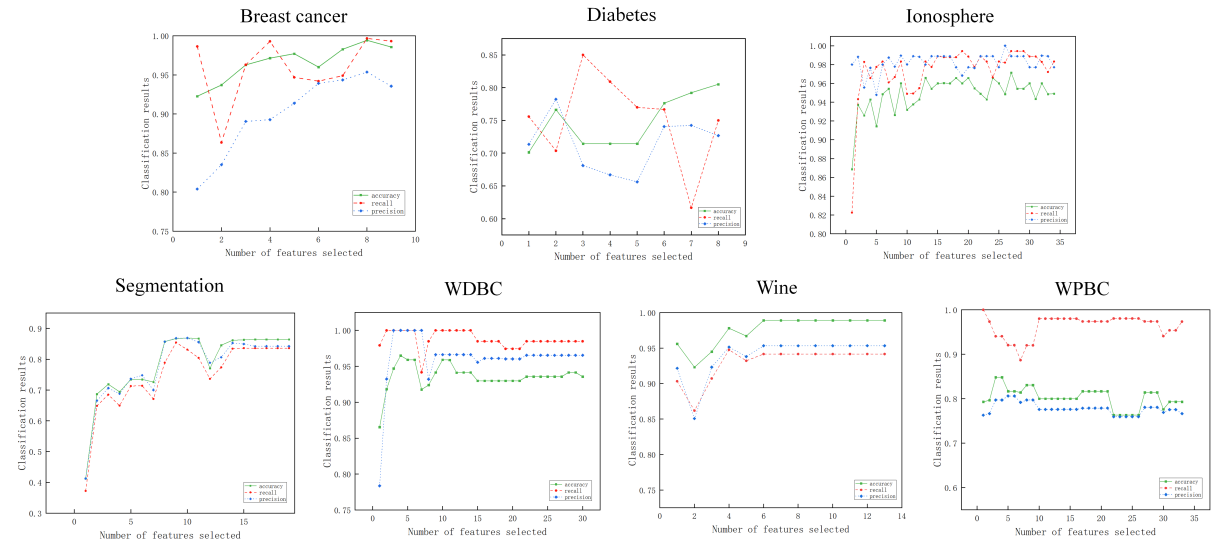

(a) Classification results with the number of features selected for KNN

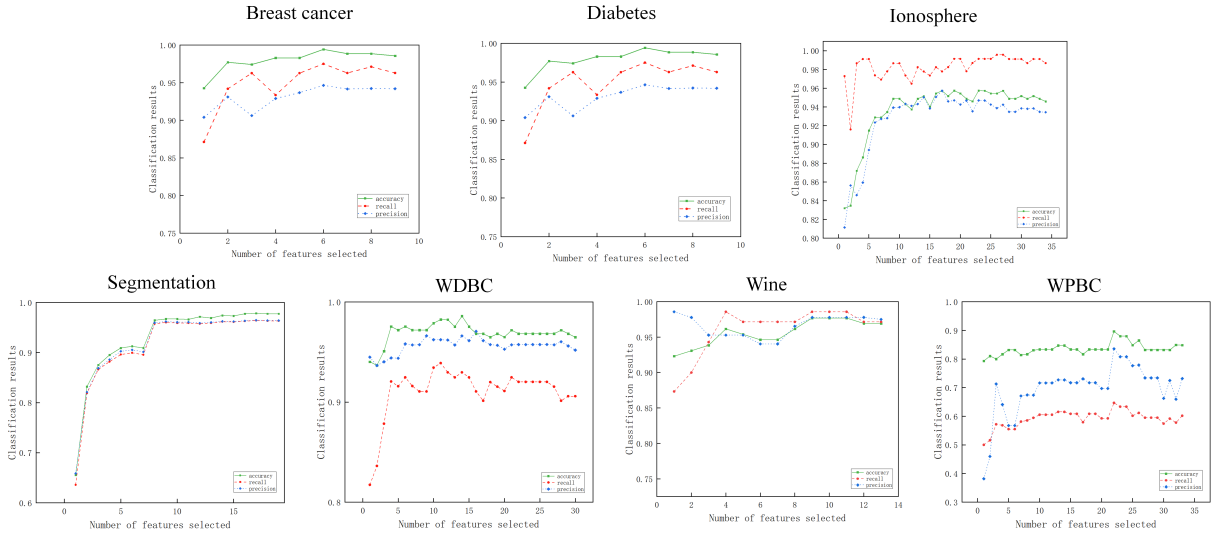

(b) Classification results with the number of features selected for SVM

Fig. 5. Results of adding classifiers step-by-step after dataset attributes are sorted.

role in D_{HTDH}. With the increase of ω, the variation in D_{HTDH} becomes more pronounced. This trend indicates that ω enables the variable-precision hybrid similarity to either emphasize or disregard certain specific features of THFCs, thereby enhancing the role of THFC structural information in D_{HTDH}.

V. Conclusion

To achieve efficient knowledge acquisition and representation in complex fuzzy environments, this study integrates HFS with TCA to construct a multi-granularity knowledge space with a dynamic adjustment mechanism. A multi-granularity knowledge acquisition approach based on THFC is introduced, facilitating the hierarchical acquisition and representation of conceptual knowledge within the context of CE. On this basis, a VP-HSM method is further developed to capture deeper differences between THFCs, thereby improving the quality of the acquired THFCs. However, practical data interactions in CE environments are often dynamic and involve complex cross-domain knowledge integration, a challenge not fully addressed by the current model. The evolving landscape of CE necessitates an adaptive framework capable of managing the complexity and timeliness of multi-domain knowledge representation in rapidly changing scenarios. Future research will focus on enhancing the adaptability and scalability of the model to effectively manage dynamic environments, enabling real-time knowledge updating, and supporting efficient processing of large-scale, multi-modal data. This will empower dynamic cross-domain knowledge transfer and application, ultimately driving advancements in various real-world domains such as smart cities, healthcare, and autonomous systems.

TABLE VII
BASELINE MODELS AND TECHNIQUES

Model	Abbrev	Used Technique	Feature Selection Level
Forward Attribute Reduction based on Variable Precision δ-Neighbourhood	FARVPDN [36]	Neighbourhood and Variable Precision Rough Sets	Global
Forward Attribute Reduction based on Variable Precision K-Nearest Neighbourhood	FARVPKNN [36]	Neighbourhood and Variable Precision Rough Sets	Global
Neighbourhood Entropy Based algorithm	NEIEN [37]	Neighbourhood Rough Sets	Global
Heuristic Algorithm Based on Neighbourhood Discrimination Index	HANDI [38]	Neighbourhood Rough Sets	Global
Neighbourhood-based Class-Specific Features Selection	NeCFeS [39]	Neighbourhood Rough Sets	Class-Specific
Granule-Specific Feature Selection Methodology	GFS [40]	Neighbourhood Rough Sets and Improved K-Nearest Neighbours Approach	Local

TABLE VIII
OVERALL CLASSIFICATION ACCURACY COMPARISON WITH KNN

No.	Ours	GFS	NeCFeS	FARVPDN	FARVPKNN	NEIEN	HANDI	Full Feature Set
1	**98.09±2.42**	97.97±1.83	95.53±2.43	-	-	-	-	96.14±2.42
2	**79.22±5.67**	78.73±5.87	74.63±4.47	72.53±4.93	72.27±5.12	-	-	74.22±3.09
3	**98.32±2.61**	98.30±2.74	98.30±2.74	97.19±5.42	96.67±7.03	94.90±6.19	96.63±5.38	94.86±6.33
4	**98.26±0.41**	97.96±0.70	95.40±1.27	-	-	92.64±1.38	93.98±0.63	95.11±1.02
5	**86.67±3.97**	82.45±3.19	77.26±3.98	-	-	75.73±2.09	72.71±4.29	76.31±3.42
6	**98.11±4.11**	94.09±4.26	91.63±4.48	88.65±4.67	89.22±4.67	-	-	83.83±6.46
7	**97.07±2.86**	96.63±2.85	95.78±2.06	96.31±2.11	95.95±2.06	96.83±2.97	95.08±2.32	97.01±2.05
Avg	**93.68**	92.30	89.79	88.67	88.53	90.03	89.47	88.21

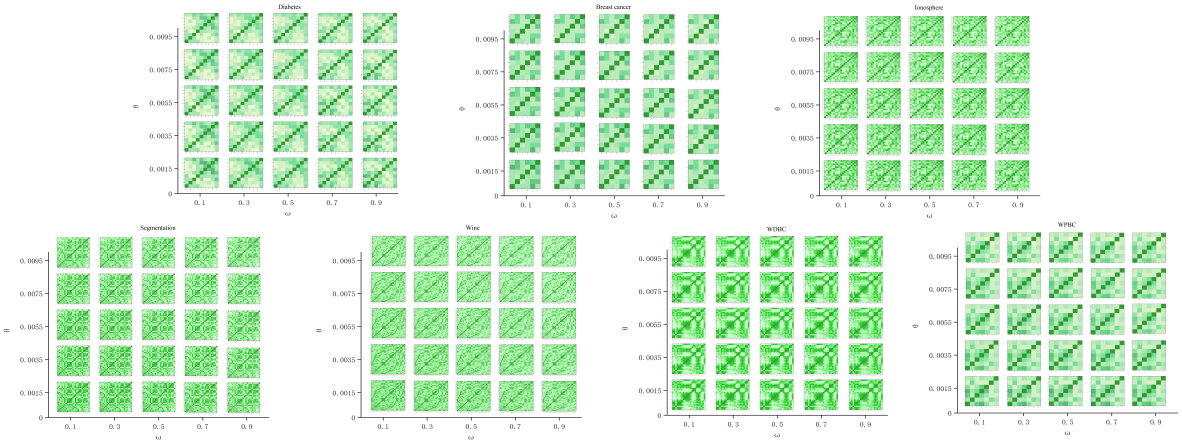

Fig. 6. Sensitivity analysis of parameters ω and θ

REFERENCES

[1] K. A. Awan, I. U. Din, A. Almogren, and J. J. P. C. Rodrigues, "Quantum-assisted intelligent decision support systems for trustworthy renewable energy management in consumer devices," *IEEE Trans. Consum. Electron.*, vol. 70, no. 2, pp. 4665-4672, May 2024.

[2] Z. Ming, H. Yu, and T. Taleb, "Federated deep reinforcement learning for prediction-based network slice mobility in 6G mobile networks," *IEEE Trans. Mob. Comput.*, vol. 23, no. 12, pp. 11937-11953, Dec. 2024.

[3] Y. Liu et al., "Topological data analysis for robust gait biometrics based on wearable sensors," *IEEE Trans. Consum. Electron.*, vol. 70, no. 2, pp. 4910-4921, May 2024.

[4] C. Wang et al., "Dependency-Aware Microservice Deployment for Edge Computing: A Deep Reinforcement Learning Approach With Network Representation," *IEEE Trans. Mob. Comput.*, vol. 23, no. 12, pp. 14737-14753, Dec. 2024.

[5] N. Chen, T. Qiu, W. Si, and D. O. Wu, "DAiMo: Motif density enhances topology robustness for highly dynamic scale-free IoT," *IEEE Trans. Mob. Comput.*, vol. 24, no. 3, pp. 2360-2375, Mar. 2025.

[6] S. P. Singh, P. Singh, D. Koundal, and M. Diwakar, "A new multi/many-objective optimization approach in wireless sensor networks for E-commerce applications," *IEEE Trans. Consum. Electron.*, vol. 70, no. 2, pp. 4848-4857, May 2024.

[7] Z. Ming et al., "Dependency-aware hybrid task offloading in mobile edge computing networks," in *Proc. IEEE 27th Int. Conf. Parallel Distrib. Syst. (ICPADS)*, Beijing, China, 2021, pp. 225-232.

[8] S. Ranjan Das et al., "Fuzzy controller designed-based multilevel inverter for power quality enhancement," *IEEE Trans. Consum. Electron.*, vol. 70, no. 2, pp. 4839-4847, May 2024.

[9] F. Lehmann and R. Wille, "A triadic approach to formal concept analysis," in *Conceptual Structures: Applications, Implementation and Theory*, G. Ellis, R. Levinson, W. Rich, and J. F. Sowa, Eds., vol. 954, pp. 400-413, May 2005.

[10] R. Wille, "Restructuring lattice theory: An approach based on hierarchies of concepts," *Order. Sets*, pp. 445-470, 1982.

[11] A. Bazin, M. Huchard, and P. Martin, "Towards analyzing variability in space and time of products from a product line using triadic concept analysis," in *Proc. 27th ACM Int. Conf. Syst. Softw. Prod. Line (SPLC '23)*, Tokyo, Japan, Aug.-Sept. 2023, pp. 85-89.

[12] Z. Li, Z. Zhang, and L. Wang, "Research on text classification algorithm based on triadic concept analysis," *Comput. Sci.*, vol. 44, no. 8, pp. 207-215, Aug. 2017.

[13] B. Ganter and S. Obiedkov, "Implications in triadic formal contexts," in *Proc. Int. Conf. Conceptual Structures (ICCS)*, Berlin, Germany, 2004, pp. 186-195.

[14] A. Bazin, T. Georges, M. Huchard, P. Martin, and C. Tibermacine, "Exploring the 3-dimensional variability of websites' user-stories using triadic concept analysis," *Int. J. Approximate Reasoning*, vol. 173, p. 109248, Oct. 2024.

[15] D. I. Ignatov, D. V. Gnatyshak, S. O. Kuznetsov, and B. G. Mirkin, "Triadic formal concept analysis and triclustering: Searching for optimal patterns," *Mach. Learn.*, vol. 101, no. 1-3, pp. 271-302, Apr. 2015.

[16] Q. Wan, J. Li and L. Wei, "Optimal granule combination selection based on multi-granularity triadic concept analysis," *Cogn. Comput.*, vol. 14, no. 6, pp. 1844-1858, Nov. 2022.

[17] S. Peng and A. Yamamoto, "Z-TCA: Fast algorithm for triadic concept analysis using zero-suppressed decision diagrams," *J. Inf. Process. Syst*, vol. 31, pp. 722-733, Jun. 2023.

[18] A. Bazin, "A triadic generalisation of the Boolean concept lattice," in D. Dürrschnabel and D. López Rodríguez, Eds., *Formal Concept Analysis, ICFCA 2023*, Lecture Notes in Computer Science, vol. 13934, pp. 95-105, Jul. 2023.

[19] P. H. Ruas, R. Missaoui, M. Song, and K. Leonard, "Mining the groceries database using triadic concept analysis," in *Proc. Int. Conf. Formal Concept Anal. (ICFCA'21)*, June 2021.

[20] M. Kaytoue, S. O. Kuznetsov, J. Macko, and A. Napoli, "Biclustering meets triadic concept analysis," *Ann. Math. Artif. Intell.*, vol. 70, no. 1-2, pp. 55-79, Feb. 2014.

[21] F. Hao, D.-S. Park, G. Min, Y.-S. Jeong, and J.-H. Park, "k-Cliques mining in dynamic social networks based on triadic formal concept analysis," *Neurocomput.*, vol. 209, pp. 57-66, Oct. 2016.

[22] X. Deng, J. Li, Y. Qian, and J. Liu, "An emerging incremental fuzzy concept-cognitive learning model based on granular computing and conceptual knowledge clustering," *IEEE Trans. Emerging Top. Comput.*, vol. 8, no. 3, pp. 2417-2432, Jun. 2024.

[23] G. F. Elhady, H. Elwahsh, M. Alsabaan, M. I. Ibrahem, and E. Shemis, "A formal fuzzy concept-based approach for association rule discovery with optimized time and storage," *Mathematics*, vol. 12, no. 23, p. 3590, Nov. 2024.

[24] R. Belohlavek and P. Osicka, "Triadic concept analysis of data with fuzzy attributes," in *Proc. IEEE Int. Conf. Granular Comput. (GrC 2010)*, San Jose, CA, USA, 2010, pp. 661-665.

[25] V. Torrá, "Hesitant fuzzy sets," *Int. J. Intell. Syst.*, vol. 25, no. 6, pp. 529-539, Mar. 2010.

[26] L. R. Dice, "Measures of the amount of ecologic association between species," *Ecology*, vol. 26, pp. 297-302, Jul. 1945.

[27] D. P. Huttenlocher, G. A. Klanderman, and W. A. Rucklidge, "Comparing images using the Hausdorff distance," *IEEE Trans. Pattern Anal. Mach. Intell.*, vol. 15, no. 9, pp. 850-863, Sep. 1993.

[28] L. A. Zadeh, "Fuzzy logic and approximate reasoning: In memory of Grigore Moisil," *Synthese*, vol. 30, pp. 407-426, Sep. 1975.

[29] M. Xia and Z. Xu, "Hesitant fuzzy information aggregation in decision making," *Int. J. Approximate Reasoning*, vol. 52, no. 3, pp. 395-407, Sep. 2011.

[30] J. Dong, S. Wan, and S.-M. Chen, "Fuzzy best-worst method based on triangular fuzzy numbers for multi-criteria decision-making," *Inf. Sci.*, vol. 547, pp. 1080-1104, 2021.

[31] Z. Su, Z. S. Xu, and S. Zhang, "Multi-attribute decision-making method based on probabilistic hesitant fuzzy entropy," in *Hesitant Fuzzy and Probabilistic Information Fusion*. Springer, Singapore, 2024, pp. 73-98.

[32] A. M. Ikotun, A. E. Ezugwu, L. Abualigah, B. Abuhaija, and J. Heming, "K-means clustering algorithms: A comprehensive review, variants analysis, and advances in the era of big data," *Inf. Sci.*, vol. 622, pp. 178-210, 2023.

[33] H. Lai, T. Huang, B. Lu, S. Zhang and R. Xiaog, "Silhouette coefficient-based weighting k-means algorithm," *Neural Comput. Appl.*, vol. 37, no. 5, pp. 3061-3075, Feb. 2025.

[34] R. Ahmadian, M. Ghatee, and J. Wahlström, "Improved user identification through calibrated Monte-Carlo dropout," *Knowl.-Based Syst.*, vol. 305, p. 112581, Dec. 2024.

[35] Z. Shao, M. N. Ahmad, and A. Javed, "Comparison of random forest and XGBoost classifiers using integrated optical and SAR features for mapping urban impervious surface," *Remote Sens.*, vol. 16, no. 4, p. 665, Feb. 2024.

[36] Q. Hu, J. Liu, and D. Yu, "Mixed feature selection based on granulation and approximation," *Knowl.-Based Syst.*, vol. 21, no. 4, pp. 294-305, May 2008.

[37] Q. Hu, L. Zhang, D. Zhang, W. Pan, S. An, and W. Pedrycz "Measuring relevance between discrete and continuous features based on neighborhood mutual information," *Expert Syst. Appl.*, vol. 38, pp. 10737-10750, Sep. 2011.

[38] C. Wang, Q. Hu, X. Wang, D. Chen, Y. Qian, and Z. Dong, "Feature selection based on neighborhood discrimination index," *IEEE Trans. Neural Networks Learn. Syst.*, vol. 29, no. 7, pp. 2986-2999, Jul. 2018.

[39] N. A. M. S. Dulanjala, Y. Li, and J. Zhang, "A class-specific feature selection and classification approach using neighborhood rough set and K-nearest neighbor theories," *Appl. Soft Comput*, vol. 143, p. 110366, Aug. 2023.

[40] N. A. M. S. Dulanjala, Y. Li, and J. Zhang, "Granule-specific feature selection for continuous data classification using neighborhood rough sets," *Expert Syst. Appl.*, vol. 238, p.121765, Mar. 2024.

[41] M. Hu, E. C. Tsang, Y. Guo, and W. Xu, "Fast and robust attribute reduction based on the separability in fuzzy decision systems," *IEEE Trans. Cybern.*, vol. 1, pp. 5559-5572, Jun. 2022.

[42] B. Sang, H. Chen, L. Yang, D. Zhou, T. Li, and W. Xu, "Incremental attribute reduction approaches for ordered data with time-evolving objects," *Knowl.-Based Syst.*, vol. 212, p. 106583, Jan. 2021.

[43] C. Wang, Y. Huang, M. Shao, and X. Fan, "Attribute reduction based on K-nearest neighborhood rough sets," *Int. J. Approximate Reasoning*, vol. 106, pp. 18–31, Mar. 2019.

[44] C. Wang, Y. Huang, M. Shao, and X. Fan, "Fuzzy rough set-based attribute reduction using distance measures," *Knowl.-Based Syst.*, vol. 164, pp. 205–212, Jan. 2019.

[45] J. Zhan and W. Xu, "Two types of coverings based multigranulation rough fuzzy sets and applications to decision making," *Artif. Intell. Rev.*, vol. 53, no. 3, pp. 167–198, Jan. 2020.

[46] X. Xin et al., "A novel attribute reduction method based on intuitionistic fuzzy three-way cognitive clustering," *Appl. Intell*, vol. 53, no. 2, pp. 1744–1758, Jan. 2023.

[47] S. Zhao, H. Chen, C. Li, X. Du, and H. Sun, "A novel approach to building a robust fuzzy rough classifier," *IEEE Trans. Fuzzy Syst.*, vol. 23, no. 4, pp. 769–786, Aug. 2015.

[48] W. Du and B. Hu, "A fast heuristic attribute reduction approach to ordered decision systems," *Eur. J. Oper. Res*, vol. 264, no. 2, pp. 440–452, Jan. 2018.

[49] Z. Huang and J. Li, "Covering based multi-granulation rough fuzzy sets with applications to feature selection," *Expert Syst. Appl.*, vol. 238, p.121908, Mar. 2024.

[50] C. Wang, Y. Huang, W. Ding, and Z. Cao, "Attribute reduction with fuzzy rough self-information measures," *Inf. Sci.*, vol. 549, pp. 68–86, Mar. 2021.